

## COBEM-2017-1362

# EQUILIBRIUM POINTS AROUND A DOUBLE ROTATING MASS DIPOLE

Santos, L. B. T.<sup>1</sup>

Prado, A. F. B. A.<sup>1</sup>

Sanchez, D. M.<sup>1</sup>

<sup>1</sup>National Institute for Space Research, INPE, São José dos Campos, SP, Brazil

leonardo.btorres@inpe.br.

antonio.prado@inpe.br.

diogo.sanchez@inpe.br.

**Abstract.** *The objective of the present work is to determine the equilibrium points and to perform an analysis of zero velocity curves in the Modified Restricted Synchronous Three-Body Problem. To perform this task, it is necessary to obtain the equations of motion, in a rotating reference frame, of a spacecraft with negligible mass that orbit around a system constituted of two massive bodies. The two massive bodies are assumed to have irregular shaped bodies and were modeled as a rotating mass dipole. The exact positions of the equilibrium points are obtained and also the values of the Jacobi constant necessary to emerge each equilibrium point. We analyzed how the position of the collinear equilibrium points vary when we modify the size and mass ratio of the two primary bodies.*

**Keywords:** *Equilibrium Points, Zero Velocity Curves, Modified Restricted Synchronous Three-Body Problem*

## 1. INTRODUCTION

It is notorious how much has grown the scientific interest in the exploration of asteroids in the last years (Pamela and Misra, 2011). Asteroid exploration has brought information about the dynamics and formation of asteroids and has entailed to a better understanding of the origin of the solar system (Pamela *et al.*, 2013).

The Exploration of asteroids and comets is a task quite challenging, due the fact of each body has its own physical characteristics of shape, density, rotation, mass distribution, et al. Then, develop a mathematical modeling of gravitation field close these bodies is a task quite complex and is necessary develop this equations encompassing the maximum of parameters possible, because several times the physical characteristics of asteroids are only discovered after an approaching spacecraft (Scheeres *et al.*, 2000).

The model adopted here assumes that the two asteroids of the binary system are modeled as a rotating mass dipole, with the purpose of representing a natural elongated body (Zeng *et al.*, 2016a). Initially, this mathematical approach in an asteroid was introduced by Zeng *et al.* (2015). More current studies of Zeng *et al.* (2016b) have adopted an improved dipole model, in which they assumed a flat dipole in an asteroid. In this study, Zeng *et al.* (2016b) found up to 13 libration points in the plane of motion. Ferrari *et al.* (2016) investigated a way to find models in the trajectories next to an asteroid system using the dipole model of rotating mass. Santos *et al.* (2017) investigated the equilibrium points and their respective zero velocity curves of an asteroid binary system, considering the restricted three-body synchronous problem, in which one of the asteroids was considered as a point mass and the second asteroid was considered as a mass dipole in rotation. In this work, we investigated the equations of motion in an asteroid binary system which the two asteroid are modeled as dipole mass in rotation.

## 2. EQUATIONS OF MOTION

The Modified Restricted Synchronous Three-Body Problem has the objective of describing the dynamics of an infinitesimal mass particle ( $P$ ) that moves under the gravitational influence of two other massive bodies ( $M_1$  and  $M_2$ ) that orbit around the center of mass of the system. The distance unit is normalized by the distance from the center of mass of the body  $M_1$  to the center of mass of the body  $M_2$ . The two primary bodies are modeled as a rotating mass dipole, i. e., each primary body is formed by two hypothetical bodies with masses  $m_{11}$  and  $m_{12}$  (for body  $M_1$ ) and  $m_{21}$  and  $m_{22}$  (for body  $M_2$ ), as shown in Figure 1.

The mass ratio is given by

$$\mu^* = \frac{m_{21}}{m_{11} + m_{12} + m_{21} + m_{22}}. \quad (1)$$

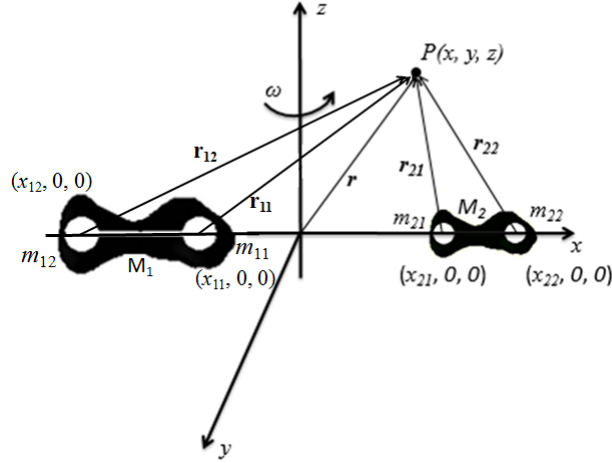


Figure 1: Representative image of the geometric shape of the system under study (not in scale).

The primary bodies are located on the  $x$ -axis, whose coordinates are given by

$$x_{11} = -2\mu^* - d_1/2, \quad (2)$$

$$x_{12} = -2\mu^* + d_1/2, \quad (3)$$

$$x_{21} = -2\mu^* - d_2/2 + 1, \quad (4)$$

$$x_{22} = -2\mu^* + d_2/2 + 1. \quad (5)$$

Here  $d_1$  is the distance between the point of mass  $m_{11}$  and  $m_{12}$  (dimension of  $M_1$ ) and  $d_2$  is the distance from the point of mass  $m_{21}$  to the point of mass  $m_{22}$  (dimension of  $M_2$ ). The equations of motion of the body of negligible mass, when viewed from a rotating reference, are given by

$$\ddot{x} - 2\dot{y} = \Omega_x, \quad (6)$$

$$\ddot{y} + 2\dot{x} = \Omega_y, \quad (7)$$

where

$$\Omega = \frac{x^2 + y^2}{2} + \frac{1 - 2\mu^*}{2r_{11}} + \frac{1 - 2\mu^*}{2r_{12}} + \frac{\mu^*}{r_{21}} + \frac{\mu^*}{r_{22}}, \quad (8)$$

with

$$r_{11} = [(x - x_{11}), y, 0]^T, \quad (9)$$

$$r_{12} = [(x - x_{12}), y, 0]^T, \quad (10)$$

$$r_{21} = [(x - x_{21}), y, 0]^T, \quad (11)$$

$$r_{22} = [(x - x_{22}), y, 0]^T, \quad (12)$$

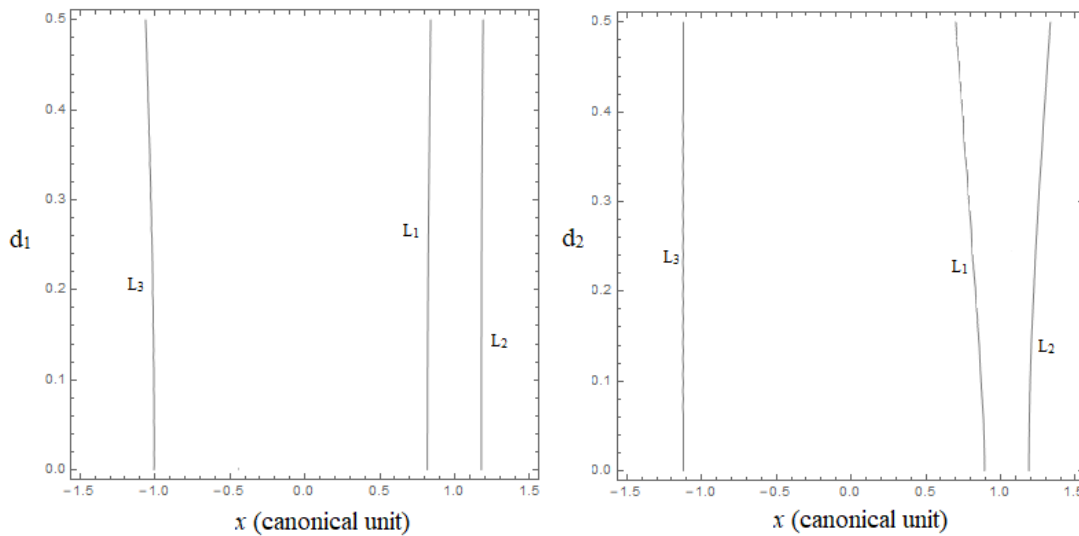
in that  $\Omega_x$  and  $\Omega_y$  are the partial derivatives of  $\Omega$  with respect to  $x$  and  $y$ , respectively.

The known *Jacobi's Integral* (Szebehely, 1967) is given by:

$$v^2 = 2\Omega - C. \quad (13)$$

Note that the Equation 13 is dependent on the function  $\Omega$  and an integration constant  $C$ , which is an integral of the equations of motion. In the literature,  $C$  is known as *Jacobi's Constant* (Dutt and Anilkumar, 2014; Ren and Shan, 2014). In this work we are assuming that the spacecraft is moving in the plane  $xy$ . Then, the Equation 13 shows us that the spacecraft velocity is a function of the position of the body in the plane, for a given numerical value of  $C$  (generated from the initial conditions) (McCuskey, 1963). It is observed that in Equation 13 there is a relation between the square of the velocity and the positions of the spacecraft in the rotating coordinate system (Molton, 1960).

In mathematical terms, the *zero velocity curve* (*ZVC*) is defined as  $2\Omega - C = 0$  (McCuskey, 1963; Szebehely, 1967). The *ZVC* expressed in Cartesian coordinates is given by



(a) Variation of collinear equilibrium points as a function of the size of the most massive primary. (b) Variation of the collinear equilibrium points as a function of the size of the less massive primary.

Figure 2: Variation of the collinear equilibrium points taking in consideration the dimension of the primary bodies.

$$\frac{x^2 + y^2}{1} + \frac{(1 - 2\mu^*)}{r_{11}} + \frac{(1 - 2\mu^*)}{r_{12}} + \frac{2\mu^*}{r_{21}} + \frac{2\mu^*}{r_{22}} = C. \quad (14)$$

The regions in which the spacecraft movement is allowed are regions where  $2U > C$ , otherwise, by Equation 13, we see that the square of the velocity would become negative, which is a physical impossibility (Szebehely, 1967).

Note that it is not possible to obtain, through this analysis, any information about the specific trajectory of the particle studied. Only the limits are determined (Szebehely, 1967). The contour curve of the equation 14 shows us the border regions where motion is allowed (Dutt and Sharma, 2011; McCuskey, 1963).

### 3. RESULTS AND DISCUSSION

Figure 2a and 2b show the x coordinates of points  $L_1$ ,  $L_2$  and  $L_3$  for different values of  $d_1$  and  $d_2$ , respectively. Note that in Figure 2a (where we vary the dimension of  $M_1$ ) the effects slightly modify the positions of  $L_3$  and  $L_1$ .  $L_2$  is far from  $M_1$ , so it remains practically constant. In Figure 2b the size of  $M_2$  was modified. Due to this fact, the points  $L_1$  and  $L_2$  have larger influence (because they are closer to the  $M_2$ ) due to the new mass distribution of this body. Notice that  $L_3$  remains practically constant.

In Figure 3, it shows how the position of the collinear points vary when we increase the mass ratio of the system.

We can note from Figure 3 that as we grow the mass ratio  $\mu^*$ , the mass of the  $M_2$  increase and the mass of  $M_1$  decrease. With this change of gravitational field of both the bodies, this causes a new configuration to be required to establish the equilibrium points. Notice that as we increase the mass of  $M_2$ , the equilibrium points that are closest to this body move away, causing the equilibrium point  $L_1$  to move to the left and the equilibrium point  $L_2$  to move to the right with respect to  $M_2$ . The equilibrium point  $L_3$  is more distant from the primary, which makes it difficult to understand the behavior of this body intuitively. Numerical evidence shows that as we increase the mass ratio, the point of equilibrium  $L_3$  moves away from the primary bodies, causing a new relation between centrifugal force and gravitational force to be necessary to annul generating a stationary point.

Some numerical tests were performed, where we consider  $\mu^* = 0.0049505$ ,  $d_1 = 0.736068$  and  $d_2 = 0.131440$ . These numerical values are based on the *Alpha - Gamma* asteroid pair of the 2001SN<sub>263</sub> asteroid system. Doing the right side of Equations 6 and 7 equal the zero and solving numerically, we find five real roots, which three of them are collinear ( $L_1$ ,  $L_2$  and  $L_3$ ) and the another two are in plane  $xy$ . The localization these equilibrium points are shown in Table 1. In Figure 4 show the positions of the equilibrium points (red) with respect to the center of mass of each primary body (black).

Some ZVC are shown in next. The color coded indicates the velocity that the spacecraft will have in each region. The color column legend shows the square velocity needed to cross from one region to another. The red regions are forbidden regions where the movement is not possible. For a spacecraft reach the in red regions with the initial conditions generated, it is necessary has velocity square negative, which is a physical impossibility.

In Figure 5 we can observe that the ZVC related the energy  $C_1 = 3.716359670795$  touches on a point called  $L_1$ . The

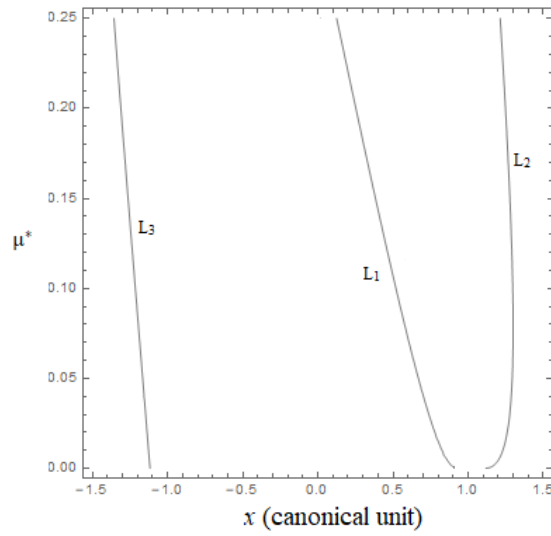


Figure 3: Positions  $\mu^*$  of collinear equilibrium points ( $L_1$ ,  $L_2$  and  $L_3$ ) for different values of  $\mu^*$ .

Table 1: The positions of equilibrium points for the studied system

		Equilibrium points
$L_1$	x	0.8621142586696
	y	0
$L_2$	x	1.2000933511901
	y	0
$L_3$	x	-1.122101868767
	y	0
$L_4$	x	0.0046508345280
	y	0.9276535170573
$L_5$	x	0.0046508345280
	y	-0.9276535170573

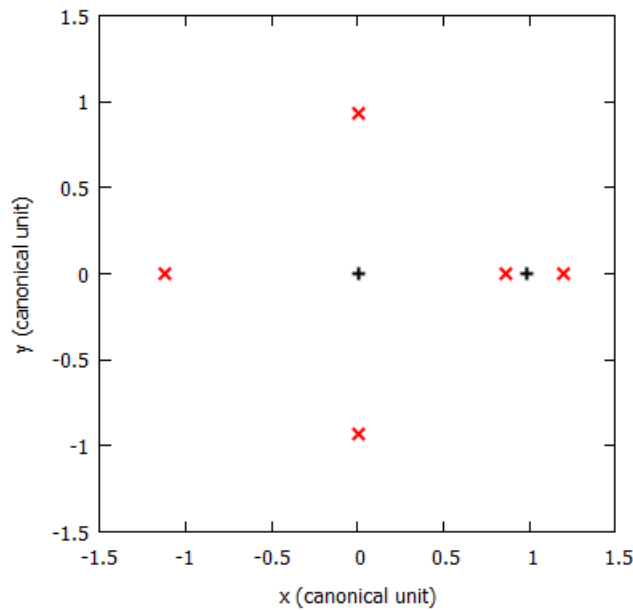


Figure 4: Positions of the equilibrium points for the system studied (red) and the positions of center of mass of primaries bodies (green).

value  $C_1$  become possible the transfer of spacecraft between  $M_1$  and  $M_2$  through of  $L_1$  point. The Figure 5b show a visual approximation of figure 5a in  $M_2$  for a better visualization of ZVC close of the  $M_2$ .

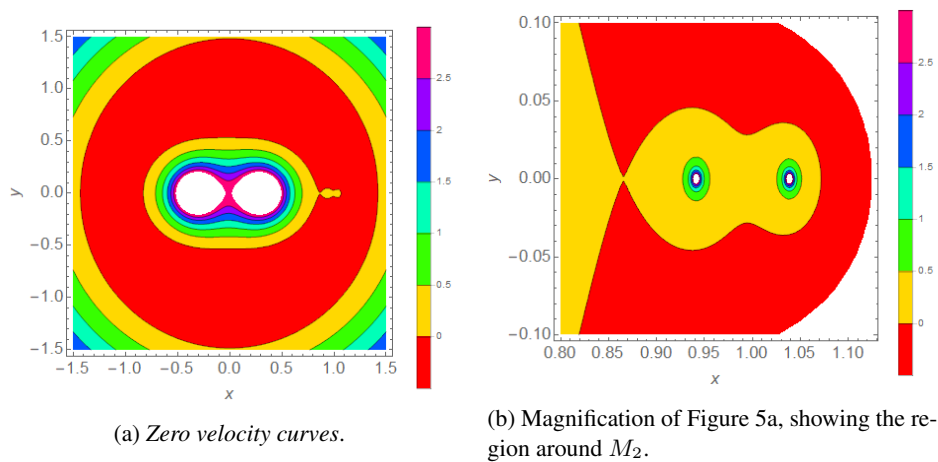


Figure 5: Zero velocity curves. The first point of contact occurs in  $C = 3.716359670795$ .

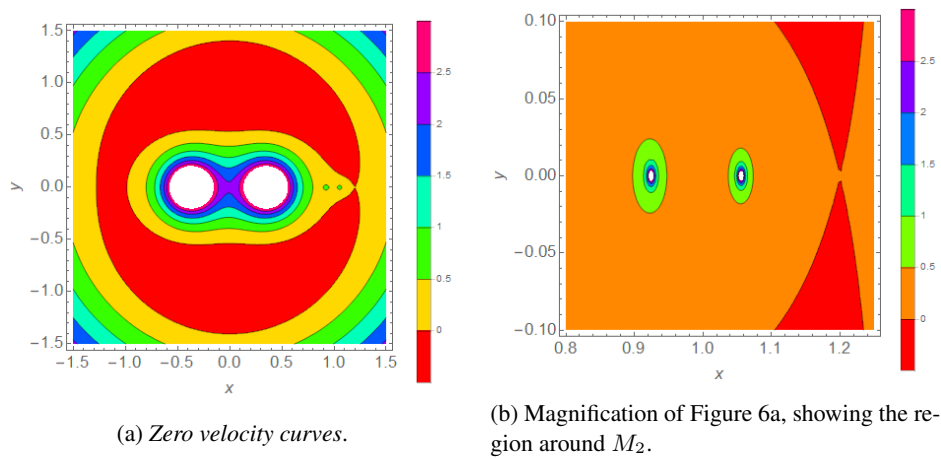


Figure 6: Zero velocity curves. The second point of contact occurs in  $C = 3.34813335305$ .

It is important observe that the spacecraft coming from  $M_1$  initially and with energy  $C_1$ , for example, just can reach the body  $M_2$  only crossing by  $L_1$  point. We can note that, by figure Plau that the transfer between the regions close  $M_1$ - $M_2$  and the infinite remains forbidden, but the transfer between  $M_1$  and  $M_2$  is possible.

Decreasing the value of  $C$ , the curves close to  $M_1$  and  $M_2$  (oval inner) becomes greater and the external curve become smaller. When the value of  $C$  arrive in  $C_2 = 3.34813335305$ , the inner oval and external oval get in touch so, we have a second contact point. This contact point is called  $L_2$ . It is possible note that for  $C = C_2$  become possible a communication between the regions close of  $M_1 - M_2$  with the infinite. The Figure 6b is a visual approximation of Figure 6a around of body  $M_2$ .

Decreasing even more the value of  $C$  until  $C_3 = 3.2678562132$ , the prohibited region reduce (red region smaller than in Figures 5 and 6) and the spacecraft has more regions for movement, as shown the Figure 7. We can note that there is a link between the region close to  $M_1$  and the infinite, but this time from left side. This contact point is called  $L_3$ .

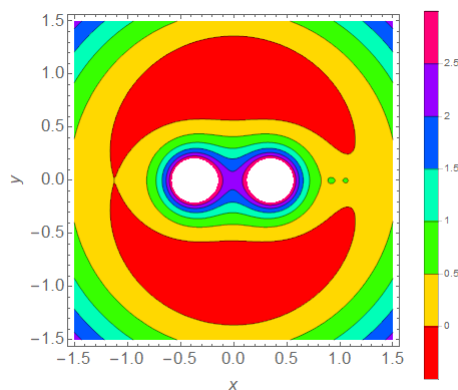


Figure 7: Zero velocity curves. The third point of contact occurs in  $C = 3.2678562132$ .

Finally, decreasing of the  $C_3$  to  $C_{4-5} = 2.85925963595$ , the forbidden region becomes smaller when compared to previous cases. Note that, only the regions around of the  $L_4$  and  $L_5$  points remain as prohibit, as shown in Figure 8. The notation  $C_{45}$  is a form abbreviated of write  $C_4$  and  $C_5$  because they have the same values.

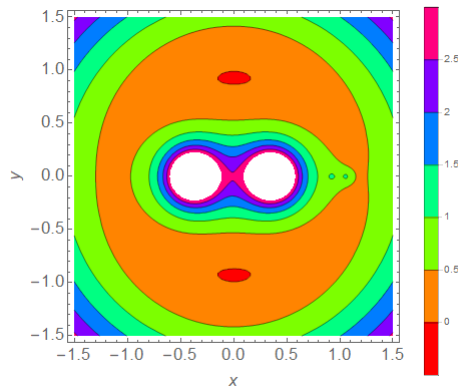


Figure 8: Zero velocity curves. The four and five points of contact occurs in  $C = 2.85925963595$ .

#### 4. CONCLUSIONS

In this work we investigate the influence that the dimension of the primary bodies and their respective masses has on the generation of the equilibrium points. For the quantitative study we realized that as we increase the dimension of  $M_2$ , the equilibrium points  $L_1$  and  $L_2$  are more influenced (because they are closer to this body) and move away from  $M_2$ . On the other hand, the point of equilibrium  $L_3$  does not undergo a considerable change by being more distant. On the other hand, when we vary the dimension of the  $M_1$ , we note a considerable change in position of equilibrium point  $L_3$ . However, the positions of equilibrium points  $L_1$  and  $L_2$  practically not alter.

It was also analyzed the influence that the mass ratio  $\mu^*$  affects the positions of the equilibrium points. Numerical evidence shows that as we increase the mass ratio (the mass of  $M_2$  becomes larger), all collinear equilibrium points move away from  $M_2$ . This is due to the fact that the gravitational field of  $M_2$  becomes greater (with the increase of  $\mu^*$ ) and with that, a new configuration is necessary to establish the points of equilibrium.

The zeros velocity curves were obtained in order to find the regions in which the spacecraft movement in the  $xy$  plane is allowed for different values of  $C$ . In this study, we verified that as we decrease the value of the Jacobi constant  $C$ , the regions where movement is permitted becomes greater.

#### 5. ACKNOWLEDGMENTS

This work was supported by grants 406841/2016-0 and 301338/2016-7 from the National Council for Scientific and Technological Development (CNPq). Also thank the grants 2016/14665-2, 2016/18418-0, 2011/08171-3, 2014/22293-2, 2014/22295-5 from São Paulo Research Foundation (FAPESP) and the financial support from the National Council for the Improvement of Higher Education (CAPES).

#### 6. REFERENCE

- Dutt, P. and Anilkumar, A.K., 2014. "Planar fly-by trajectories to moon in the restricted three-body problem." *Advances in Space Research*, Vol. 54, pp. 2050–2058.
- Dutt, P. and Sharma, R., 2011. "Evolution of periodic orbits near the lagrangian point 12." *Advances in Space Research*, Vol. 47, pp. 1894–1904.
- Ferrari, F., Lavagna, M. and Howell, K., 2016. "Dynamical model of binary asteroid systems through patched three-body problems." *Celestial Mechanics and Dynamical Astronomy*, Vol. 125, No. 4, pp. 413–433.
- McCuskey, S.W., 1963. *Introduction to Celestial Mechanics*. Addison-Wesley Publishing Company, USA, 1st edition.
- Molton, F.R., 1960. *An Introduction to Celestial Mechanics*. The Macmillan Company, New York, 4th edition.
- Pamela, W. and Misra, A.K., 2011. *Dynamics and Control of a Spacecraft Near Binary Asteroids*. The Macmillan Company, New York, 5th edition.
- Pamela, W., Misra, A.K. and Keshmiri, M., 2013. "On the planar motion in the full two-body problem with inertial symmetry." *Celestial Mechanics and Dynamical Astronomy*, Vol. 117, pp. 263–277.
- Ren, Y. and Shan, J., 2014. "Low-energy lunar transfers using spatial transit orbits." *Communications in Nonlinear Science and Numerical Simulation*, Vol. 19, pp. 554–569.
- Santos, L.B.T., Prado, A.F.B.A. and Sanchez, D.M., 2017. "Equilibrium points in the restricted synchronous three-

bodyproblem using a mass dipole model.” *Astrophysics and Space Science*, Vol. 362, No. 61, p. 60.

Scheeres, D.J., Williams, B.G. and Miller, J.K., 2000. “Evaluation of the dynamic environment of an asteroid: Applications to 433 eros”. *Journal of Guidance, Control and Dynamics*, Vol. 23, No. 3, pp. 466–475.

Szebehely, V., 1967. *Theory of Orbits*. Academic press., New York and London.

Zeng, X.Y., Li, J. and Baoyin, H., 2016a. “Updated rotating mass dipole with oblateness of one primary (i): Equilibria in the equator and their stability.” *Astrophysics and Space Science*, Vol. 361, No. 1, p. 14.

Zeng, X.Y. *et al.*, 2015. “Study on the connection between the rotating mass dipole and natural elongated bodies. astrophysics and space science.” *Astrophysics and Space Science*, Vol. 356, pp. 29–42.

Zeng, X., Liu, X. and Li, J., 2016b. “Extension of the rotating dipole model with oblateness of both primaries.” *Research in Astron. Astrophys.* First online.

## 7. RESPONSIBILITY NOTICE

The authors are the only responsible for the printed material included in this paper.